7

Three- Dimensional Numerical Simulation of Cohesive Sediment Transport in Natural Lakes

Xiaobo Chao and Yafei Jia
The University of Mississippi
USA

1. Introduction

Sediment has been identified as one of the leading nonpoint-source pollutants. Most sediments are transported into surface water bodies from agricultural lands and watersheds through runoff, and greatly affect the surface water quality. Sediment particles will change channel topography and play an important role in affecting water quality physically or chemically by the pollutants, nutrients and pesticides they carried. Shallow lakes in the Southern U.S. are often surrounded by agriculture lands. The suspended sediments in these shallow lakes are normally very fine, and they can be classified as cohesive sediments.

The basic processes involved in cohesive sediment transport, such as flocculation, deposition, erosion, consolidation, etc., have been studied by many scientists. Burban et al. (1990) presented a formula to calculate the settling velocity of flocs in fresh water based on laboratory experiments. Thorn (1981), Ziegler and Nisbet (1995), Li and Mehta (1998) established several empirical formulas for settling velocity of flocs by considering the effects of sediment size, sediment concentration, salinity, turbulence intensity, and bed shear stress. Krone (1962) and Mehta and Partheniades (1975) investigated deposition of cohesive sediment and proposed formulas to estimate deposition rates. Partheniades (1965) proposed a formula to calculate the erosion rate of cohesive sediment. Hamm and Migniot (1994) studied the consolidation of cohesive bed material using an approach of three stage process.

In recent decades, some researchers have studied the cohesive sediment transport in rivers, lakes, and coastal waters using numerical models. Willis and Krishnappan (2004) reviewed a number of numerical models and gave an overview of the knowledge base required for modeling cohesive sediment transport in river flow. Nicholson and O'Connor (1986) developed a 3D cohesive sediment transport model using a splitting method in conjunction with a characteristics technique and a mixed explicit-implicit finite difference approach. Ziegler and Nisbet (1995), Bailey and Hamilton (1997), and Wu and Wang (2004) developed several two-dimensional (2D) depth-averaged models to simulate cohesive sediment transport. Liu (2007) developed a vertical (laterally integrated) two-dimensional model to simulate the cohesive sediment transport in Danshuei River estuary by considering the effects of reservoir construction upstream of the river. Normant (2000), Jin and Ji (2004) proposed 3D layer models to simulate the cohesive sediment transport in estuaries and lakes, respectively.

Sediment erosion, transport and suspension often result from turbulent flows. In inland lakes, however, the water flow is often dominated by wind, and the wave induced by wind

generates the most dynamic conditions along shorelines. Jin and Sun (2007) studied the flow circulation, wave dynamics and their impacts on sediment resuspension and vertical mixing in Lake Okeechobee based on field measurements. Their results show that wave action is the dominant factor in sediment re-suspension in that lake. Cozar et al. (2005) presented empirical correlations between total turbidity and wind speed based on the field observations. They also obtained an empirical formula to calculate the suspended sediment concentration using wind speed and water depth. Some researchers have shown that sediment resuspension in shallow lakes is primarily a result of wave action (Luettich et al 1990; Hawley and Lesht 1992). Field observations in Deep Hollow Lake, a shallow oxbow lake in Mississippi showed that during the period from October to December of 1999, the concentration of suspended sediment in the lake varied from 20 to 90 mg/l, even though there was no runoff discharged into the lake during this time (Rebich and Knight 2001). It was apparent that these levels of suspended sediment concentration reflected the influence of wind-induced currents and waves.

This paper presents a 3D model developed based on the mass transport equation for simulating the concentration distribution of cohesive sediment in shallow lakes. It was assumed that low concentration of sediment does not affect the motion of flow, therefore, the decoupled approach was used to calculate the flow field and sediment transport separately. Flow information such as velocity fields, free surface elevations, and eddy viscosity parameters were obtained from a three dimensional hydrodynamic model CCHE3D (Jia et al 2001), and processes of flocculation, deposition, erosion, etc., were considered in the cohesive sediment transport simulation. Because the wind-driven hydrodynamics are considered as important features for sediment transport and re-suspension in lakes, in this flow model, the bottom shear stresses induced by currents and waves were calculated.

This model was first verified by a simple mathematic solution consisting of the movement of a non-conservative tracer in a prismatic channel with uniform flow, and the numerical results agreed well with the analytical solutions. Then it was applied to Deep Hollow Lake, a shallow oxbow lake in Mississippi. Simulated sediment concentrations were compared with available field observations. The trend obtained from the numerical model was generally in good agreement with the observations. It was found that without considering the effect of wind-induced wave, a numerical model can never capture the observed suspended sediment distribution.

This paper presents detailed technical information on cohesive sediment transport in lakes. The background and objectives of this paper are introduced in Section 1. Section 2 describes the general cohesive sediment transport processes in a lake, including flocculation, deposition, erosion, consolidation, etc. Section 3 describes the numerical model for simulating the cohesive sediment transport. Section 4 describes the effect of wind-driven flow and wind-induced wave on sediment transport. Section 5 presents two cases for model verifications. Section 6 provides an application case of the model to a shallow lake in Mississippi. The discussions and conclusions are described in Section 7 and Section 8, respectively.

2. General cohesive sediment transport processes in a lake

The general processes governing cohesive sediment transport in lakes are flocculation, settling, deposition, erosion, consolidation, etc.

2.1 Flocculation

Due to the action of electrostatical forces, the individual fine sediment particles may move toward each other and form the so called flocs/aggregates when they collide. This process is called flocculation, and it is affected by sediment size, sediment concentration, turbulence intensity, temperature, organic matters, etc. (Thorn, 1981; Mehta, 1986; McConnachie, 1991). Flocculation becomes weaker when sediment size increases. In general, high sediment concentration would enhance flocculation as the collision is intensified. The turbulence of flow also affects flocculation. In the range of low shear stress, turbulence increases the chance of collision among sediment particles so that flocculation increases. When the shear stress exceeds the critical level, flocculation may reduce as turbulence increases. Temperature has a significant influence on flocculation. High temperature intensifies flocculation as the thermal motions of ions increase.

2.2 Settling velocity

In natural lakes, the settling velocity of cohesive sediment depends on the floc size, concentration of particles, organic content of the sediment, etc. The flocculation process is dynamic and complex. The median floc diameter can be estimated from the following experiment-based equation (Lick and Lick 1988; Gailani et al 1991):

$$d_m = \left(\frac{\alpha_0}{CG} \right)^{0.5} \tag{1}$$

where d_m = median floc diameter (cm); G = fluid shear stress(dyne/cm^2); C = concentration of sediment (g/cm^3); and α_0 = experimentally determined constant. For fine-grained cohesive sediments in freshwater, $\alpha_0 = 10^{-8} gm^2 / cm^3 / s^2$.

Based on laboratory experiments on flocculated, cohesive sediments in freshwater, Burban et al. (1990) proposed a formula to calculate the settling velocity:

$$w_s = a d_m^b \tag{2}$$

where $a = 9.6 \times 10^{-4} (CG)^{-0.85}$ and $b = -\left[0.8 + 0.5 \log(CG - 7.5 \times 10^{-6}) \right]$

Eqs (1) and (2) address the effects of sediment concentration and flow shear stress on flocculation, and they can be used for lake simulation.

2.3 Deposition and erosion of cohesive sediment

When the bottom shear stress is less than the critical shear stress for deposition, sediment can settle down on the bed. Based on Krone (1962) and Mehta and Partheniades (1975), the deposition rate (D_b) can be calculated by:

$$D_b = \begin{cases} 0 & \tau_b > \tau_{cd} \\ w_s C \left(1 - \dfrac{\tau_b}{\tau_{cd}} \right) & \tau_b \le \tau_{cd} \end{cases} \tag{3}$$

where τ_b = bed shear stress (N/m^2); τ_{cd} = critical shear stress for deposition (N/m^2).

When the bottom shear stress is greater than the critical shear stress for erosion, cohesive sediment can be eroded. There are three erosion modes proposed by Mehta (1986). The first erosion mode is the flocs or aggregates that are eroded from bed in particles. The second mode is the mass erosion due to the failure of sediment bed along a plane below the bed surface, and the sediment above the plane is eroded in layers. The third mode is the entrainment of sediment when a fluid mud is formed at the water-sediment interface. Erosion rate is generally expressed by Partheniades (1965)

$$E_b = \begin{cases} 0 & \tau_b < \tau_{ce} \\ M\left(\dfrac{\tau_b}{\tau_{ce}} - 1\right) & \tau_b \geq \tau_{ce} \end{cases} \tag{4}$$

where τ_{ce} = critical shear stress for erosion (N/m^2); M = erodibility coefficient related to the sediment properties, the reported values are in the range of 0.00001 to 0.0004 kg/m^2/s (van Rijn 1989).

Gailani et al.(1991) and Ziegler and Nisbet (1995) studied the cohesive sediment transport in lakes and reservoirs, and found that the erosion rate is a power function of the dimensionless excessive shear stress:

$$E_b = \frac{a_0}{t_d^m}\left(\frac{\tau_b - \tau_{ce}}{\tau_{ce}}\right)^n \tag{5}$$

where a_0= site-specific coefficient; t_d = time after deposition (day); m and n = coefficients, m is about 2, and n is 2~3.

2.4 Consolidation of cohesive sediment

Consolidation is an important process in cohesive sediment transport. It is a compaction process of deposited material under the influence of gravity and water pressure with simultaneous expulsion of pore water and a gain in strength of bed material. Consolidation is generally classified in three stages. The first stage is the settlement of flocs to form a fluid mud, which occurs within several hours of deposition. The second stage is the escaping of pore water, which happens in one or two days. The third stage is the gelling of clay, which may take years to reach the final state.

The degree of consolidation is affected by the sediment size, the mineralogical composition, the thickness of deposit layer, etc. It was observed that the dry bed density varies along the depth below the bed surface, and the relationship between the bed density and consolidation time can be estimated as (Hayter, 1983):

$$\frac{\bar{\rho}_d}{\bar{\rho}_{d\infty}} = 1 - ae^{-pt}dc/t\,dc\infty \tag{6}$$

where $\bar{\rho}_d$ = mean dry bed density; $\bar{\rho}_{d\infty}$ = final dry bed density; t_{dc}= consolidation time; $t_{dc\infty}$ = final consolidation time; parameters a and p are taken as 0.845 and 6.576, respectively.

Lane and Koelzer (1953) proposed a formula to estimate the dry bed density in consolidation processes:

$$\rho_d = \rho_{d0} + \beta \log t_{dc} \tag{7}$$

where ρ_d = dry bed density; ρ_{d0}= dry bed density after one year of consolidation; t_{dc}= consolidation time; and β = coefficient.
Consolidation affects the bed shear strength and also the erosion rate. The critical shear stress for erosion τ_{ce} can be estimated by considering the effect of consolidation (Nicholson and O'Connor, 1986):

$$\tau_{ce} = \tau_{ce0} + k_t(\rho_d - \rho_{d0})^{nt} \tag{8}$$

where τ_{ce0}=critical shear stress at the initial period of bed formation; ρ_d = dry bed density; ρ_{d0} = dry bed density at the initial period of bed formation; k_t and n_t are empirical parameters with the values of 0.00037 and 1.5, respectively.

3. Hydrodynamic and cohesive sediment transport models

3.1 Governing equations

A three-dimensional flow and sediment transport model is needed to study the cohesive sediment transport in surface waters. The CCHE3D hydrodynamic model (Jia et al. 2001, and 2005) and the associated transport model (Chao et al. 2006, 2009) were applied and are presented in this paper. CCHE3D is a three-dimensional model that can be used to simulate unsteady turbulent flows with irregular boundaries and free surfaces. It is a finite element model utilizing a special method based on the collocation approach called the efficient element method. This model has been successfully applied to analyze wind-driven flow, turbulent flow fields in scour holes and around a submerged training structure in a meander bend. The transport model was developed on the finite element platform of CCHE3D flow model.
The governing equations of the three-dimensional unsteady hydrodynamic model can be written as follows:

$$\frac{\partial u_i}{\partial x_i} = 0 \tag{9}$$

$$\frac{\partial u_i}{\partial t} + u_j \frac{\partial u_i}{\partial x_j} = -\frac{1}{\rho}\frac{\partial p}{\partial x_i} + \frac{\partial}{\partial x_j}\left(\nu \frac{\partial u_i}{\partial x_j} - \overline{u_i' u_j'}\right) + f_i \tag{10}$$

where u_i $(i=1,2,3)$ = Reynolds-averaged flow velocities (u, v, w) in Cartesian coordinate system (x, y, z); t = time; ρ = water density; p = pressure; ν = fluid kinematic viscosity; $-\overline{u_i' u_j'}$ =Reynolds stress; and f_i = body force terms.
The free surface elevation (η) is computed using the following equation:

$$\frac{\partial \eta}{\partial t} + u_f \frac{\partial \eta}{\partial x} + v_f \frac{\partial \eta}{\partial y} - w_f = 0 \tag{11}$$

where u_f, v_f and w_f = velocities at the free surface; η = surface water elevation.
The governing equation for cohesive sediment transport is based on the three-dimensional mass transport equation:

$$\frac{\partial C}{\partial t} + \frac{\partial (uC)}{\partial x} + \frac{\partial (vC)}{\partial y} + \frac{\partial (w - w_s)C}{\partial z} = \frac{\partial}{\partial x}(D_x \frac{\partial C}{\partial x}) + \frac{\partial}{\partial y}(D_y \frac{\partial C}{\partial y}) + \frac{\partial}{\partial z}(D_z \frac{\partial C}{\partial z}) \tag{12}$$

in which C= concentration of cohesive sediment; D_x, D_y and D_z = mixing coefficients in x, y and z directions, respectively; w_s = settling velocity.

3.2 Boundary conditions

To solve the 3D cohesive sediment transport equation (12), the boundary conditions at the free surface and bottom are needed. At the free surface, the vertical sediment flux is zero and the following condition is applied:

$$w_s C + D_z \frac{\partial C}{\partial z} = 0 \tag{13}$$

At the bottom, the following condition is applied:

$$w_s C + D_z \frac{\partial C}{\partial z} = D_b - E_b \tag{14}$$

where D_b and E_b = deposition rate and erosion (resuspension) rate at bottom, respectively (kg/m²/s). They can be calculated using Eqs. (3) and (4).

3.3 Numerical simulation

In the CCHE3D model, the turbulence Reynolds stresses in Eq. (10) are approximated according to Bousinesq's Assumption and they are related to the rate of the strains of flow fields and a coefficient of eddy viscosity. There are several turbulence closure schemes available in the CCHE3D model, including two zero equation models (parabolic eddy viscosity model and mixing length model), a k-ε model and a nonlinear k-ε model. In this model, an upwinding scheme is adopted to eliminate oscillations due to advection, and a convective interpolation function is used for this purpose due to its simplicity for the implicit time marching scheme which was adopted in this model to solve the unsteady equations. The numerical scheme of this approach is the second order. The velocity correction method is applied to solve the dynamic pressure and enforce mass conservation. Provisional velocities are solved first without the pressure term, and the final solution of the velocity is obtained by correcting the provisional velocities with the pressure solution (Jia et al., 2001). The system of the algebraic equations is solved using the Strongly Implicit Procedure (SIP) method (Stone 1968).

The decoupled approach for flow and sediment simulation has been widely adopted in the solution of many real-life engineering problems (Wu, 2008). In general, for the lower flow regime with low sediment concentration (lower than 300 mg/l), the decoupled approach is appropriate (Willis and Krishnappan, 2004; Wu, 2008). In this study, the flow and sediment simulations were decoupled and the flow fields, including water elevation, velocity components, and eddy viscosity parameters were obtained using the CCHE3D free surface hydrodynamic model (Jia et al., 2001 and 2005). After obtaining flow fields, the settling velocity, and boundary conditions of surface and bottom, the distribution of cohesive sediment in the water column were computed by solving the 3D mass transport equation (Eq. 12) numerically. The numerical method used for solving Eq. (12) is consistent with the method employed in the CCHE3D model.

4. The effects of wind-driven flow and wind-induced wave on cohesive sediment transport

In natural lakes, wind stress and wind-induced wave are important driving forces of lake water flows. The water flows coming into and/or out of the lake are normally insignificant to the volume of the water in the lake; in comparison, the current induced by wind are much stronger and have complex distributions, because the wind forcing is acting on the entire water surface. Therefore, the flow circulations within lakes are often influenced by wind. In addition, temperature and salinity stratifications and the Coriolis force, etc., also play important roles. It is observed that in many closed inland lakes, the temperature stratification is minimal, the flow and sediment transport is dominated by wind-induced currents, and the sediment resuspension is primarily affected by wind-induced waves.

4.1 Wind-driven flow

When vertical flow circulation is formed by wind stress, the turbulence stress in the flow balances the momentum of the flow taking from the wind forcing. Because the turbulence stress is related to eddy viscosity coefficient, the distribution of vertical eddy viscosity is required for simulating the wind driven flow. A parabolic eddy viscosity distribution was proposed by Tsanis (1989) based on the assumption of a double logarithmic velocity profile. The vertical eddy viscosity was expressed as:

$$\nu_t = \frac{\lambda u_{*_s}}{H}(z + z_b)(z_s + H - z) \tag{15}$$

in which λ= numerical parameter; z_b and z_s = characteristic lengths determined at bottom and surface, respectively; u_{*s} = surface shear velocity; H = water depth. To use this formula, three parameters, λ, z_b and z_s have to be determined. For some real cases with very small water depths, using this formula to calculate eddy viscosity may cause some problems.

Koutitas and O'Connor (1980) proposed two formulas to calculate the eddy viscosity based on a one-equation turbulence model. Their formulas were:

$$\nu_t = \nu_{t,\max}\eta(2 - \eta) \qquad (0 \le \eta \le 0.5) \tag{16}$$

$$\nu_t = \nu_{t,\max}(1 - \eta)(5\eta - 1) \qquad (0.5 < \eta \le 1) \tag{17}$$

where

$$\nu_{t,\max} = \lambda u_{*_s} 0.105 H 0.3^{-0.25} = 0.142\lambda u_{*_s} H \tag{18}$$

in which, λ = numerical parameter; η = non-dimensional elevation, $\eta = z / H$.

In this paper, a new formula was proposed based on experimental measurements conducted in a laboratory flume with steady-state wind driven flow reported by Koutitas and O'Connor (1980). The form of eddy viscosity was borrowed from Koutitas and O'Connor's assumption (Eq. 16 and 17) and expressed as:

$$\nu_t = \nu_{t,\max} f(\eta) \tag{19}$$

Based on measured data, a formula was obtained to express the vertical eddy viscosity:

$$\nu_t = \nu_{t,\max}\eta(-3.24\eta^2 + 2.78\eta + 0.62) \tag{20}$$

Fig. 1 shows the vertical distributions of eddy viscosity obtained from experimental measurements and formulas provided by Tsanis (Eq.15), Koutitas (Eq. 16 and 17), and our model (Eq.20). Since there is no measured value for eddy viscosity at the water surface, the surface eddy viscosity may be estimated using Eq. 20. This formula can be used to calculate the eddy viscosity over the full range of water depth.

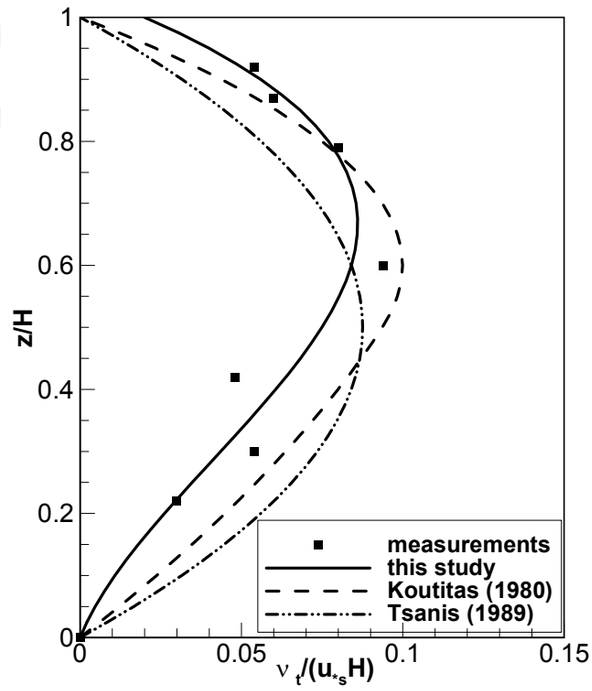

Fig. 1. Comparison of vertical eddy viscosity formulas and experimental data

The wind shear stresses (τ_{wx} and τ_{wy}) at the free surface are expressed by

$$\tau_{wx} = \rho_a C_d U_{wind} \sqrt{U_{wind}^2 + V_{wind}^2} \tag{21}$$

$$\tau_{wy} = \rho_a C_d V_{wind} \sqrt{U_{wind}^2 + V_{wind}^2} \tag{22}$$

where ρ_a = air density; U_{wind} and V_{wind} = wind velocity components at 10 m elevation in x and y directions, respectively. Although the drag coefficient C_d may vary with wind speed (Koutitas and O'Connor 1980; Jin et al. 2000), for simplicity, many researchers assumed the drag coefficient was a constant on the order of 10^{-3} (Huang and Spaulding 1995; Bailey and Hamilton 1997; Rueda and Schladow 2003; Kocyigit and Kocyigit 2004). In this study, C_d was set to 1.0×10^{-3}, and this value is applicable for simulating the wind driven flow in Deep Hollow Lake (Chao et al 2004).

In this paper, the eddy viscosity was calculated using Eq. 20. The wind shear stresses were calculated from wind speeds (Eq.21 and 22) and set as flow boundary condition at the free surface. Using the developed numerical model, the flow fields induced by wind can be simulated. Those flow fields determined the cohesive sediment transport in a water body.

4.2 Bed shear stress

In natural lakes, the interactions of high-frequency surface wind-induced waves with relatively low-frequency currents determine the structures of near-bed shear stresses in water bodies. Both mechanisms of shear stresses are considered in calculating sediment deposition rate and erosion rate. If the wave and current boundary layers are turbulent, the combined wave-current bottom shear stress is a highly nonlinear function which can be estimated based on the Grant-Madsen wave-current model (Grant and Madsen 1979; Glenn and Grant 1987).

Many investigations have shown the shear stresses exerted by circulatory currents are generally much smaller than those due to waves in shallow lakes, and can be neglected (Luettich et al. 1990; Hawley and Lesht 1992; Hamilton and Mitchell 1996). In this paper, the total bottom shear stress is computed as the sum of wave and current shear stresses (van Rijn, 1993; Hawley and Lesht, 1992; Teeter et al., 2001). In this study, the wind-induced current is not very strong, so the bed shear stresses τ_b due to waves and currents can be treated separately, and τ_b in Eq.(3) and (4) is calculated by

$$\tau_b = \tau_w + \tau_c \tag{23}$$

where τ_w and τ_c = bottom shear stresses due to waves and currents, respectively.

The current shear stress τ_c at the bottom is calculated by:

$$\tau_c = \rho u_*^2 \tag{24}$$

in which u_* = shear velocity at bottom, and can be calculated by the log law:

$$\frac{u}{u_*} = \frac{1}{\kappa} ln\left(\frac{z}{z_o}\right) \tag{25}$$

in which κ = von Karman constant; z_0= roughness length which is a function of the bed roughness height k_s and shear velocity u_* :

$$z_o = 0.11\frac{\nu}{u_*} \qquad u_* k_s/\nu \le 5 \tag{26}$$

$$z_o = 0.0333 k_s \qquad u_* k_s/\nu \ge 70 \tag{27}$$

$$z_o = 0.11\frac{v}{u_*} + 0.0333 k_s \qquad 5 < u_* k_s/\nu < 70 \tag{28}$$

The bottom shear stress generated by wind-induced waves can be calculated by the laminar wave theory (Luettich et al. 1990):

$$\tau_w = \frac{1}{2}\rho f_w U_b^2 \tag{29}$$

in which U_b = maximum wave orbital velocity; and f_w = friction factor. Based on the wave boundary layer (Dyer, 1986), f_w is given by

$$f_w = 2\left(\frac{U_b A_b}{\nu}\right)^{-0.5} \tag{30}$$

in which A_b = maximum wave orbital amplitude. A_b and U_b are given by CERC (1984):

$$A_b = \frac{1}{2\sinh(2\pi d / L)} \tag{31}$$

$$U_b = \frac{\pi H}{T\sinh(2\pi d / L)} \tag{32}$$

So the bottom shear stress generated by wind waves τ_w can be calculated by

$$\tau_w = H\left[\rho\frac{\left(\nu\left(\frac{2\pi}{T}\right)^3\right)^{0.5}}{2\sinh\left(\frac{2\pi d}{L}\right)}\right] \tag{33}$$

where H = wave height(m); d = water depth (m); T = wave period (s); and L = wave length (m). In shallow lakes, the wind-induced wave parameters, such as wave height H, wave period T and wave length L can be estimated using the following empirical formulas (CERC 1984):

$$\frac{gH}{U_w^2} = 0.283\tanh\left[0.53\left(\frac{gd}{U_w^2}\right)^{3/4}\right]\tanh\left[\frac{0.00565\left(\frac{gF}{U_w^2}\right)^{1/2}}{\tanh\left[0.53\left(\frac{gd}{U_w^2}\right)^{3/8}\right]}\right] \tag{34}$$

$$\frac{gT}{U_w} = 7.54\tanh\left[0.833\left(\frac{gd}{U_w^2}\right)^{3/8}\right]\tanh\left[\frac{0.0379\left(\frac{gF}{U_w^2}\right)^{1/2}}{\tanh\left[0.833\left(\frac{gd}{U_w^2}\right)^{3/8}\right]}\right] \tag{35}$$

$$L = \frac{gT^2}{2\pi}\tanh\frac{2\pi d}{L} \tag{36}$$

where g = acceleration of gravity(m/s^2); U_w = wind speed at 10 m above the water surface(m/s); and F = fetch length of wind (m).

5. Model verification

5.1 Verification of the model for wind-driven flow

The actual process of wind-shear-driven flow is very complicated: waves are generated by the wind; the main flow near the free surface moves in the wind direction while the flow near the bed may move in the opposite direction to offset the surface flow. In order to check the correctness of the computational models and assure the errors between the observation and prediction are not due to mathematic derivation and numerical coding, verification of the computational models using analytical solutions is necessary. Because it is not possible to have analytical solutions under general conditions, analytical solutions obtained for a simplified problem are often used for model verification.

This test case concerns the simulation of a steady vertical two-dimensional wind-induced flow in a uniform closed rectangular basin of constant water depth with a known, constant vertical eddy viscosity coefficient. Using the no-slip condition at the channel bed, the analytical solution for the horizontal velocity component was given by Koutitas and O'Connor (1980).

In the numerical simulation, the water depth was set as 40 m, and three meshes with different vertical elements set as 6, 11 and 21 points, were used for model simulation. The other parameters were adopted as follows: water density ρ_w=1000 kg/m^3; eddy viscosity ν_t =0.03 m^2/s, wind shear stress τ_{wx}=0.1 N/m^2; and gravitational acceleration g=9.817 m/s^2. Fig. 2 shows the comparison of the analytical solution and the numerical simulation results for velocity profiles along the water depth. All of the results using the three meshes are in good agreement with the analytical solution. The surface maximum velocity u_{max} obtained from numerical model using three meshes are 0.0337 *m/s*, 0.0334 *m/s* and 0.0334 *m/s*, respectively, and the result obtained from the analytical solution is 0.03333 *m/s.* At the depth of (*2/3*)*H,* the flow changes directions from positive to negative. The local maximum negative velocity *(u=1/3 u_{max})* is located at the depth of (*1/3*)*H.*

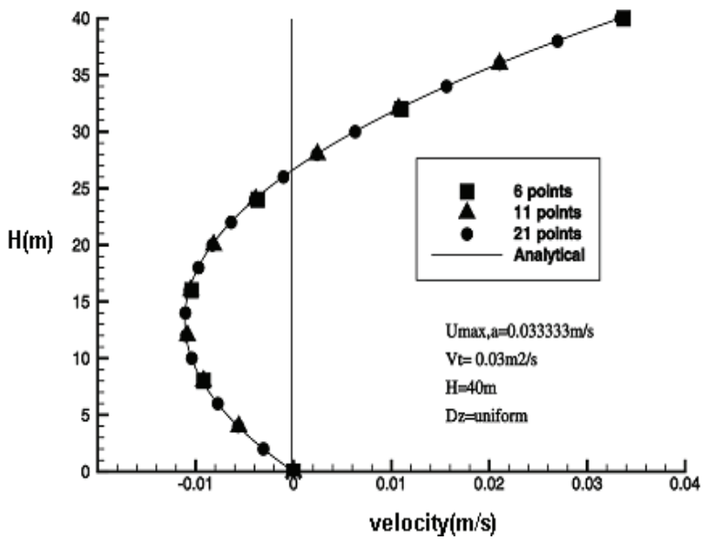

Fig. 2. Comparison of the analytical solution and the numerical simulation of wind-driven flow

5.2 Verification for the mass transport model

The proposed cohesive sediment transport model was tested against an analytical solution for predicting the concentrations of a non-conservative substance in a hypothetical one-dimensional river flow with constant depth and velocity. A continuous source of a non-conservative substance was placed at the upstream end of a straight channel for a finite period of time, τ (Fig. 3). Under the unsteady condition, the concentration of the substance throughout the river can be expressed as:

$$\frac{\partial C_s}{\partial t} + U\frac{\partial C_s}{\partial x} = D_x\frac{\partial^2 C_s}{\partial x^2} - K_d C_s \tag{37}$$

where U = velocity; C_s = concentration of substance; D_x = mixing coefficient; and K_d = decay rate. An analytical solution given by Chapra (1997) is:

$$C_s(x,t) = \frac{C_0}{2}\left[\exp\left(\frac{Ux}{2D_x}(1-\Gamma)\right)erfc\left(\frac{x-Ut\Gamma}{2\sqrt{D_x t}}\right) + \exp\left(\frac{Ux}{2D_x}(1+\Gamma)\right)erfc\left(\frac{x+Ut\Gamma}{2\sqrt{D_x t}}\right)\right] \quad (t<\tau) \tag{38}$$

$$C_s(x,t) = \frac{C_0}{2}\left\{\exp\left(\frac{Ux}{2D_x}(1-\Gamma)\right)\left[erfc\left(\frac{x-Ut\Gamma}{2\sqrt{D_x t}}\right) - erfc\left(\frac{x-U(t-\tau)\Gamma}{2\sqrt{D_x(t-\tau)}}\right)\right] + \exp\left(\frac{Ux}{2D_x}(1+\Gamma)\right)\left[erfc\left(\frac{x+Ut\Gamma}{2\sqrt{D_x t}}\right) - erfc\left(\frac{x+U(t-\tau)\Gamma}{2\sqrt{D_x(t-\tau)}}\right)\right]\right\} \quad (t > \tau) \tag{39}$$

where $\Gamma = \sqrt{1+4\eta}$, and $\eta = \frac{K_d D_x}{U^2}$. For the river conditions shown in Fig. 3, with a depth of 10 m, u = 0.03m/s, D_x = 30 m²/s, τ = 6 hr, and the values of K_d = 0, 1.0/day and 2.0/day, respectively. Fig. 4 shows the time series of concentration at the section x = 2000 m obtained by the numerical model and analytical solution. The maximum error is less than 2%.

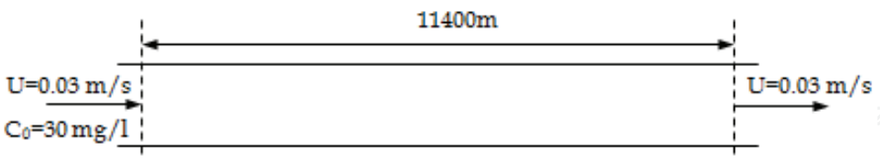

Fig. 3. Test river for verification case

6. Model application to Deep Hollow Lake

6.1 Study area

Fig.5 shows the study area of Deep Hollow Lake. It has a typical morphology of an oxbow lake, with a length of about 1 km and a width of about 100 m. Lake water depth ranges from 0.5 m to 2.6 m, with the greatest depth in the middle. The lake receives runoff from a two square kilometer watershed that is heavily cultivated. This lake is located in Leflore County, Mississippi, and it was one of three natural lakes in the Mississippi River Alluvial Plain monitored under the interagency Mississippi Delta Management System Evaluation Area Project (MDMSEA). This project was part of a national program designed to evaluate the

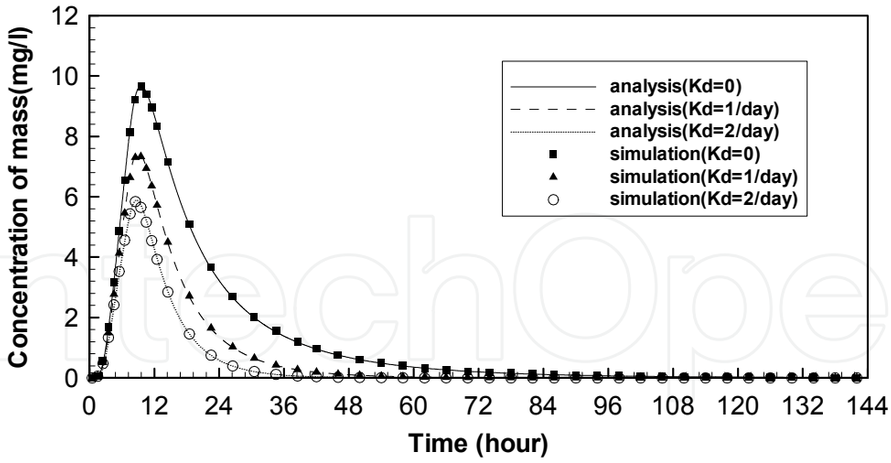

Fig. 4. The time series of concentration at the section x = 2000m obtained from the numerical model and analytical solution

impact of agricultural practices on water quality and to develop best management practices (BMPs) to minimize adverse effects of agricultural activities on water quality of the lakes (Rebich and Knight, 2001; Locke 2004).

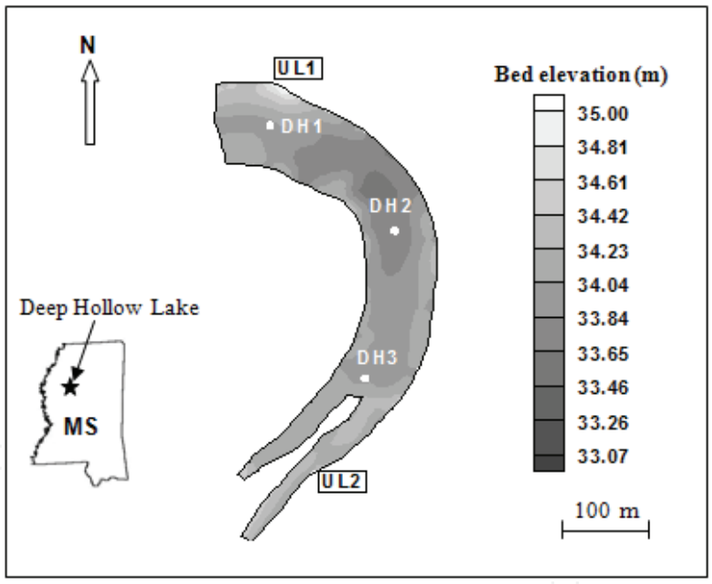

Fig. 5. Study Site – Deep Hollow Lake

Weekly or biweekly samples of suspended sediment, nutrients, chlorophyll, bacteria, and other selected water quality variables were collected at Stations DH1, DH2 and DH3. Two of the major inflows, located at the Stations UL1 and UL2, were monitored for water quality and quantity by the U.S. Geological Survey. The nutrient concentrations in Deep Hollow Lake are mainly dependent on the fertilizer loadings in the surrounding farmland and the quantity of runoff. Field measurements show that the concentrations of nitrate and ammonia in the lake are very low, while the concentration of phosphorus is relatively high in comparison with other areas nationwide. Suspended sediment concentrations are

relatively high, exceeding published levels known to adversely impact fish growth and health (Rebich and Knight, 2001).

Based on bathymetric data, the computational domain was discretized into a structured finite element mesh using the CCHE Mesh Generator (Zhang 2002). In the horizontal plane, the irregular computational domain was represented by a 95 × 20 mesh. In the vertical direction, the domain was divided into 8 layers with finer spacing near the bed. This grid system has been successfully applied to simulate the flow and water quality in Deep Hollow Lake (Chao et al 2004 and 2006).

6.2 Model calibration

The cohesive sediment transport model was calibrated using weekly field data and analysis of lake water samples obtained between October and December, 1999. Although there was no water flow discharged into the lake during this period, the measured suspended sediment concentrations varied from 20 to 90 mg/l (Rebich and Knight, 2001). Evidently these concentrations were reflecting the influence of wind-induced currents and waves.

Based on field measurements conducted by the USDA, National Sedimentation Laboratory, the median diameter of sediment particles d_{50} in Deep Hollow Lake is ~ $2.5\times10^{-6} - 3\times10^{-6}$ m, well within the clay size range. The settling velocity of cohesive sediment was estimated using Eqs.(1) and (2) to be on the order of 10^{-4} m/s.

Fig. 6 shows observed wind speeds and directions at the 3-meter level during the calibration period. The flow currents induced by wind during this period were obtained by the CCHE3D hydrodynamic model. The flow patterns were mainly determined by wind stresses. Wind shear on the surface of the lake forced upper layers of the water column to move in the direction of the wind, and produced opposite movement in deeper layers. The flow model was first calibrated using field measurements obtained from Deep Hollow Lake using an Acoustic Doppler Current Profiler (Shields et al. 2003), and then it was applied to simulate the flow fields during the simulation period. The surface velocities were measured using floating tracer particles. Fig. 7 shows the comparison of simulated flow currents with field measurements. It can be seen that the numerical results are generally in good agreement with field measurements. Figs. 8a and 8b show the simulated flow currents during the calibration period.

In order to test the model simulation capability of mass transport under the wind driven condition, the field observation data of a slug–injection dye tracer study at Deep Hollow Lake conducted by National Sedimentation Laboratory was compared with model results (Chao et al. 2007). Fig. 9 shows the dye concentration distribution in the lake at a depth of 1.25m and 24hr after injection. During this period, the prevailing wind direction was from southwest to northeast. The computed dye concentrations are generally in good agreement with the observations.

The bed shear stress generated by wind-induced currents can be obtained using CCHE3D, and the values of the bed shear stress were in the order of 10^{-3} N/m^2. Computed results show that the bed shear stresses generated by wind waves were generally in the ranges of 10^{-2} to 10^{-3} N/m^2, about one order of magnitude greater than those produced by wind-induced currents. Evidently, sediment in Deep Hollow Lake is primarily re-suspended by wind wave action and transported primarily by currents induced by wind.

For the sediment resuspension or deposition to occur, bed shear stress must be greater than the critical erosion shear stress (τ_{ce}), or less than the critical deposition shear stress (τ_{cd}),

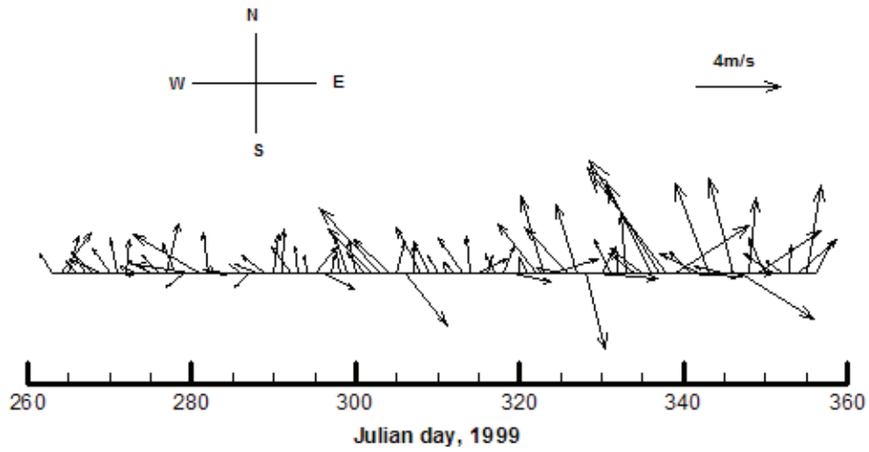

Fig. 6. Observed wind speeds and directions at 3m level

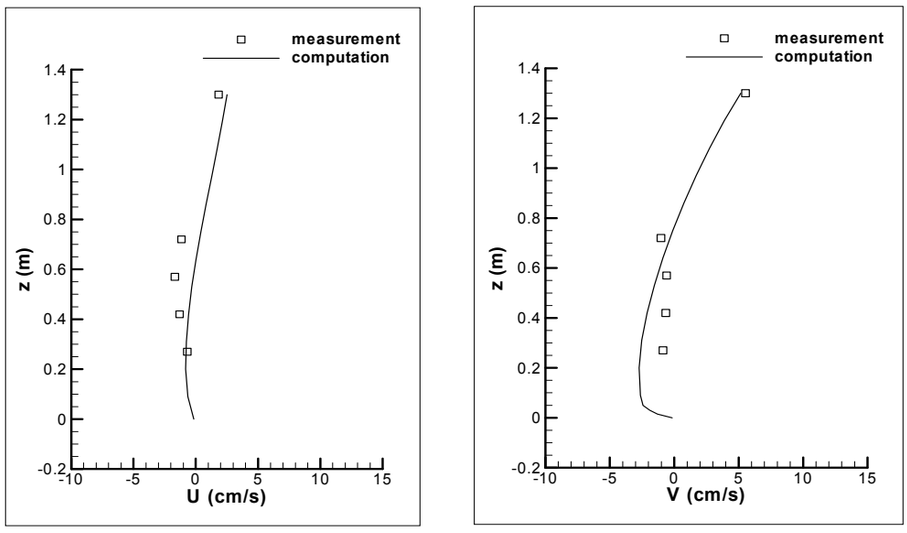

Fig. 7. Observed and simulated velocity at Station DH1 (11:05 am, 11/12/03)

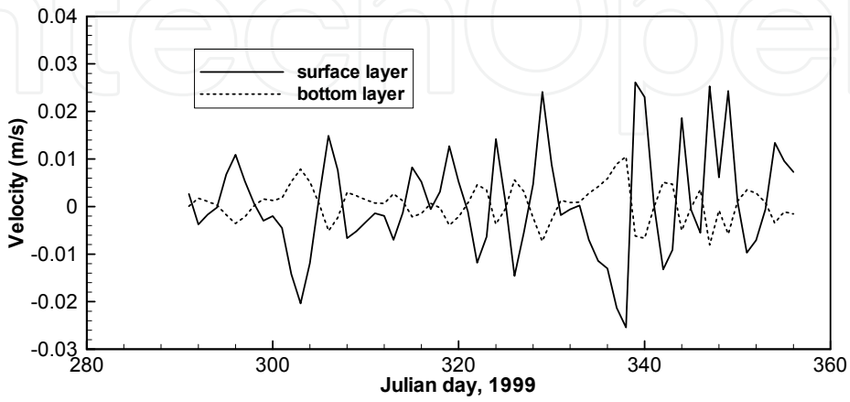

Fig. 8a. Simulated east-west velocity components at Station DH1

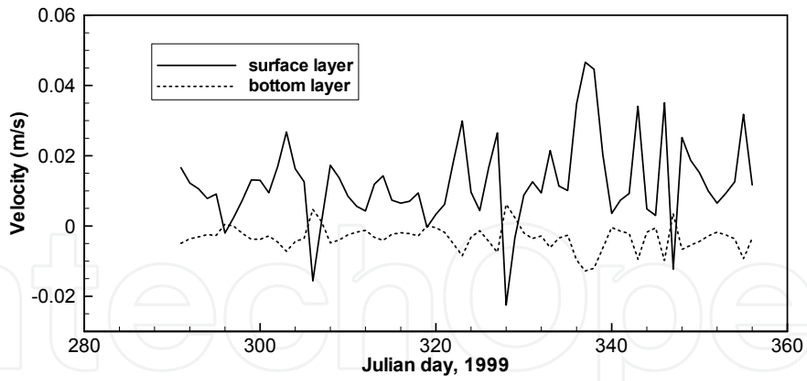

Fig. 8b. Simulated north-south velocity components at Station DH1

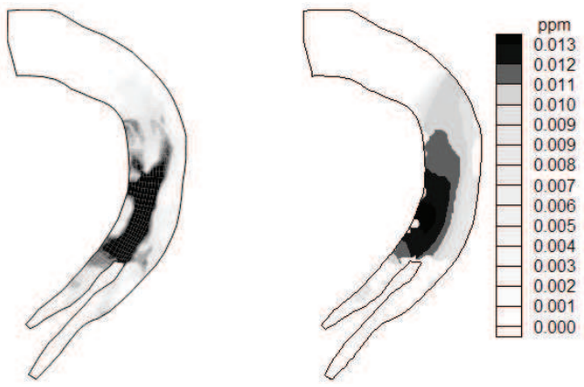

measurements numerical solution

Fig. 9. Dye concentration distribution at Deep Hollow Lake (T=1500 minutes, H=1.25m)

respectively. Previous studies on cohesive sediment transport in lakes, have reported that values for τ_{ce} and τ_{cd} in the range of 0.009 N/m² to 0.25 N/m² and 0 to 0.18 N/m², respectively (Lou et al. 2000; Hamilton and Mitchell 1996; Ziegler and Nisbet 1995; Mehta and Partheniades 1975).

Since these two critical stresses were not measured in Deep Hollow Lake, sensitivity analyses were conducted to determine the values of critical shear stresses for erosion and deposition (τ_{ce}, τ_{cd}). Fig. 10 and Fig.11 show the cohesive sediment concentration at DH2 Station under different values of τ_{ce} and τ_{cd}, respectively. In general, the suspended sediment concentrations increase with the decrease of critical shear stresses for erosion and deposition (τ_{ce}, τ_{cd}). By comparing the numerical results of sediment concentration with field measurements shown on Fig. 10 and Fig. 11, the values of τ_{ce} and τ_{cd} for the model calibration run were set to 0.02 N/m² and 0.01 N/m², respectively.

Fig. 12 and Fig.13 show the simulated and observed concentrations of cohesive sediment at Stations DH1 and DH2. Some differences between measurement and prediction may arise from the fact that measurements occurred weekly while the time step for the simulation was 300 seconds. However, trends obtained from the numerical model were generally in agreement with the observations. Fig. 12 and Fig.13 also show the concentration of cohesive sediment at Stations DH1 and DH2 without considering the effects of wind-induced waves. Big errors between simulations and measurements were observed without considering the wave effects.

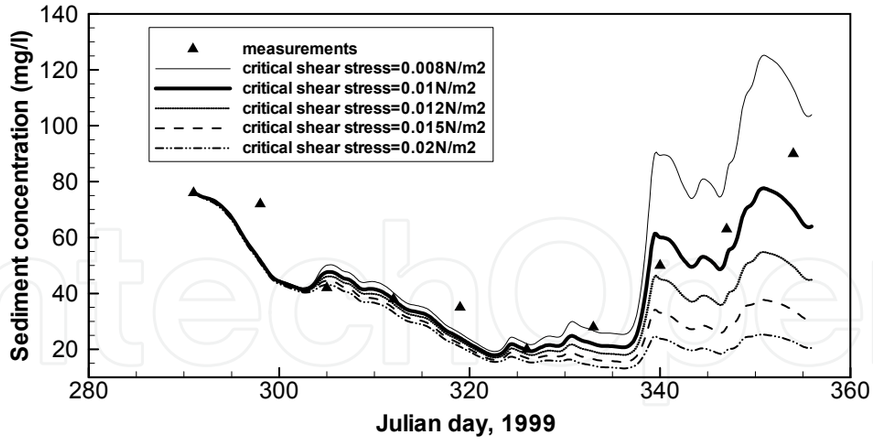

Fig. 10. The time series of sediment concentration with different critical shear stress for deposition at Station DH2

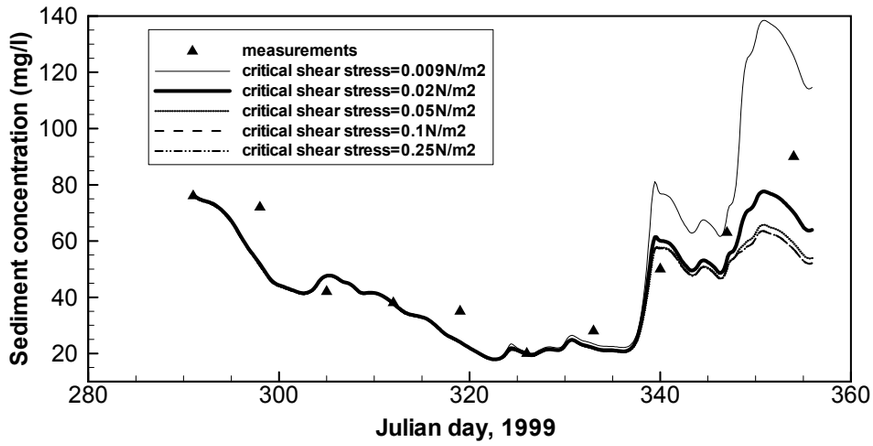

Fig. 11. The time series of sediment concentration with different critical shear stress for erosion at Station DH2

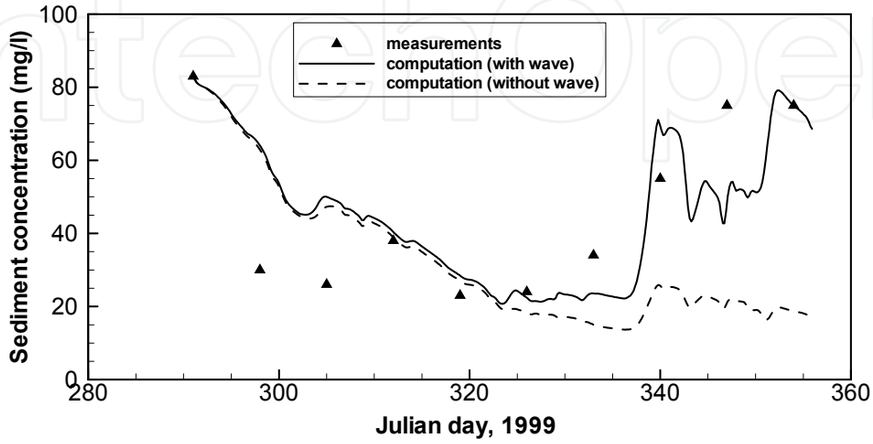

Fig. 12. Suspended sediment concentration at Station DH1

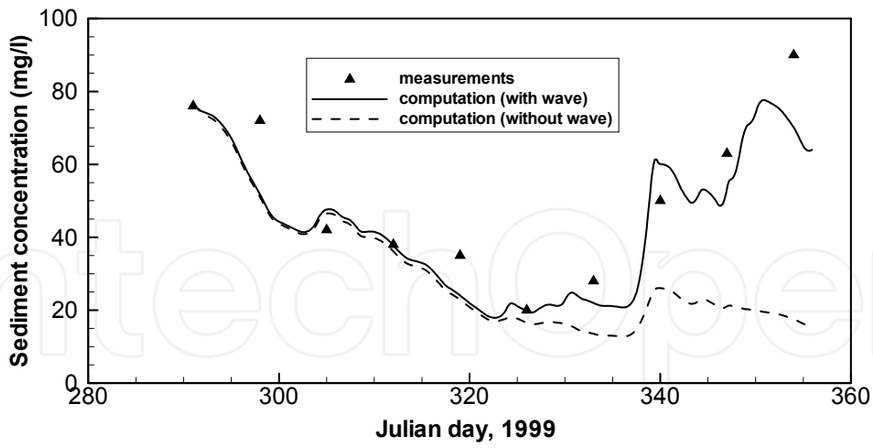

Fig. 13. Suspended sediment concentration at Station DH2

A set of statistics was used to assess the performance of the model (Stow et al 2003). The mean error and root mean square error (RMSE) of the model predictions and observations are summarized in Table 1. Without considering the effects of wind-induced waves, the percentages of mean errors of cohesive sediment concentration at Stations DH1 and DH2 were increased from 8% to 24%, and from 11% to 38%, respectively; Root Mean Square Errors (RMSE) of cohesive sediment concentration for DH1 and DH2 Stations were increased from 15.2 to 29.5 mg/l, and from 11.7 to 29.4 mg/l, respectively.

Fig. 6 shows that from the beginning to Julian day 322, winds were not strong and wind wave effects were negligible. After the Julian day 322, wind speeds (3m above surface) were generally greater than 4 m/s, and the major direction was southeast. Due to the relative long wind fetch and shallow water depth at the upstream end of the lake, the wave – induced bottom shear stress was greater there and caused sediment resuspension in that area. As shown in Figs. 12 and 13, wind-driven waves played a significant role in sediment resuspension and the maximum additional sediment concentration due to wave effects could reach 60 mg/l.

Stations	Mean observations(mg/l)	Wave Effects	Mean prediction (mg/l)	Mean error(mg/l)	Mean error(%)	Root mean square error
DH1	46.30	Yes	50.02	3.72	8	15.2
		No	35.27	-11.03	-24	29.5
DH2	51.4	Yes	45.69	-5.71	-11	11.7
		No	32.09	-19.31	-38	29.4

Table 1. Calibration statistics of cohesive sediment concentration in Deep Hollow Lake

6.3 Model validation

The period from August to October 2000 was chosen for model validation. Just as for the calibration period, there was no water flow discharged into the lake during this period, and wind and wind-induced waves were the major factors for cohesive sediment movement.

Parameter values in the simulation were based on those calibrated values during the period of October to December, 1999. Fig. 14 shows the observed wind speeds and directions at the 3-meter level during the validation period. Fig. 15 shows the simulated and observed concentrations of cohesive sediment at Station DH2. Although there were some differences between measurement and prediction, trends and quantities of concentration of cohesive sediment from the numerical model were generally in agreement with the observations.

During the validation period, the effects of wind-induced waves were not as significant as in the calibration period. It can be seen from Fig.15, due to the effects of wind-induced waves, the sediment concentrations have some differences after the Julian day 270. Fig. 14 shows strong northwest (NW) winds (>5m/s) occurred for a few days during a period from Julian day 270 to 290. However, due to the relative short wind fetch, the wave–induced bottom shear stresses were not large, and sediment resuspension due to the wave effects may not be so significant. In another short period from Julian day 310 to 318, wind speeds were generally greater than 4 m/s, and the major direction was southeast (SE). Due to the relative long wind fetch and shallow water depth at the upstream of the lake, the wave–induced bottom shear stresses were great enough to cause sediment resuspension in that area. Both field measurements and numerical results show sediment concentration in this period increased gradually.

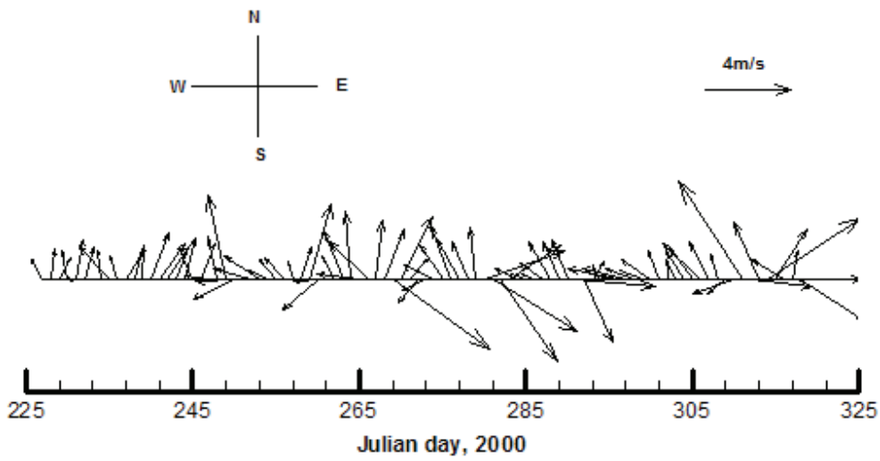

Fig. 14. Observed wind speeds and directions at 3-meter level

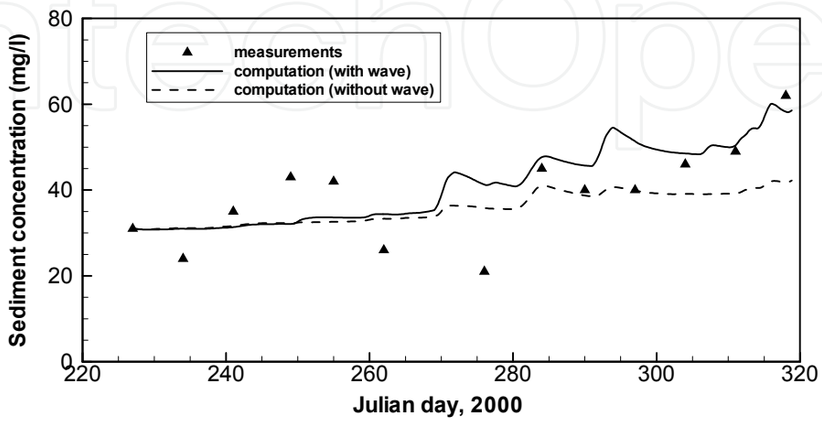

Fig. 15. Suspended sediment concentration at Station DH2

7. Discussion

7.1 Effects of wind induced current and wave on sediment resuspension in Deep Hollow Lake

Field observations of Deep Hollow Lake indicated that the suspended sediment concentration is affected strongly by wind-induced currents and waves. To better understand this dynamic process in Deep Hollow Lake, wind-induced currents and waves were simulated for some hypothetical cases. It was assumed the wind speed at 10-meter level was 10m/s, and the directions were S, SE, SW, N, NE and NW. Table 2 shows the comparisons of simulation results of wind-induced currents and waves for all the cases. On the water surface, the mean velocities of wind-induced currents were from 0.078 to 0.083 m/s, about 0.8% of wind speed. The maximum bottom shear stresses due to current were from 0.02 to 0.024 N/m^2, slightly greater than the critical shear stress (0.02 N/m^2). In most areas of the lake, the wind current-induced bottom shear stresses were less than critical shear stress for erosion. For the S, SE and SW wind, computed results show that the maximum bed shear stresses generated by wind waves were generally about one order of magnitude greater than bed shear stresses due to currents. For the N, NE and NW wind, the maximum bed shear stresses due to waves were about 2 to 4 times greater than those due to currents. So in Deep Hollow Lake, if there is no runoff discharged into the lake, suspended sediment is transported primarily by wind- induced currents and resuspended primarily by wind wave action.

Figure 16 shows regions where the wind wave-induced bottom shear stress exceeds critical shear stress for erosion under the actions of wind from S, SE, SW, N, NE, and NW directions in Deep Hollow Lake. Those regions might be the potential sediment resuspension area in the lake due to the effects of wind- induced waves.

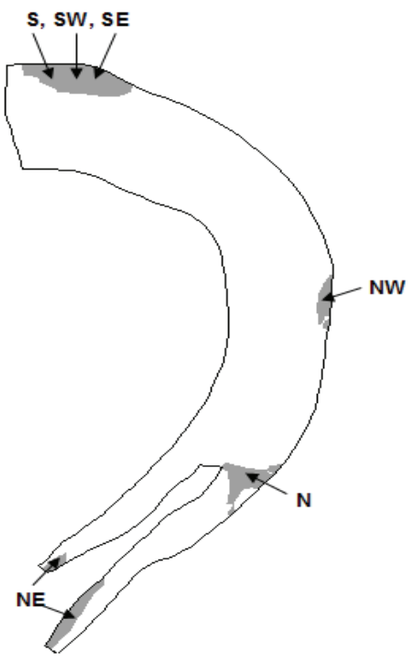

Fig. 16. Regions where the wind wave-induced bottom shear stresses exceed critical shear stress under the actions of wind from S, SE, SW, N, NE, and NW directions

Wind direction	Wind speed *(m/s)*	$\tau_{w,max}$ *(N/m²)*	$\tau_{c,max}$*(N/m²)*	$\overline{u}_s$ *(m/s)*
S	10	0.2	0.024	0.078
SE	10	0.423	0.023	0.083
SW	10	0.213	0.02	0.079
N	10	0.065	0.024	0.080
NE	10	0.095	0.024	0.081
NW	10	0.033	0.021	0.081

Table 2. Simulation results for wind-induced currents and waves for all the cases.

In Table 2, $\tau_{w,max}$ = maximum wind wave induced bottom shear stress; $\tau_{c,max}$ = maximum current induced bottom shear stress; and $\overline{u}_s$ = averaged surface velocity.

8. Conclusions

A three-dimensional numerical model for simulating the concentration of cohesive sediment influenced by currents and wind waves in natural lakes has been presented. The bottom shear stresses induced by wind driven flow and waves were calculated, and the processes of resuspension, deposition, settling, etc., were considered. This model was first verified using analytical solutions of flow and mass transport, and then it was applied to simulate the concentrations of suspended sediment in a closed inland lake, Deep Hollow. Trends and magnitudes of cohesive sediment concentration obtained from the numerical model were generally in good agreement with field observations. Field measurements and model results show that the sediment is resuspended primarily by the actions of wind waves and transported by wind driven flow in the lake. This model provides a useful tool for predicting the cohesive sediment resuspension and transportation in a natural lake, which is an important component for studying the lake water quality and ecology system.

9. Acknowledgments

This work is a result of research sponsored by the USDA-ARS National Sedimentation Laboratory and the University of Mississippi. The suggestions and advice provided by Dr. F. Douglas Shields, Jr and Dr. Charles M. Cooper of the USDA-ARS National Sedimentation Laboratory, and Dr. Sam, S.Y. Wang, Dr. Weiming Wu, Dr. Yan Ding and Ms. Kathy McCombs of NCCHE, The University of Mississippi are highly appreciated.

10. References

Bailey, M.C. and Hamilton D.P. (1997). Wind induced sediment resuspension: a lake-wide model. *Ecological Modeling*, 99, 217-228.

Burban, P.Y., Xu, Y.J., Mcneil, J. and Lick, W.(1990). Settling speeds of flocs in fresh water and seawater. *J.Geophys. Res.*,95(C10), 18213-18220.

CERC (1984). *Shore Protection Manual,* Vol.1, US Army Corp of Engineering, Vicksburg, MS, USA.

Chao, X., Jia, Y. and Shields, D.(2004). Three dimensional numerical simulation of flow and mass transport in a shallow oxbow lake. *Proc., World Water & Environmental Resources Congress 2004*, ASCE, Resyon, Va. (CD-Rom).

Chao, X., Jia, Y., Cooper, C.M., Shields Jr., F.D., and Wang, S.S.Y. (2006). Development and application of a phosphorus model for a shallow oxbow lake. *J. Environmental Engineering*, Vol. 132, No.11, 1498–1507.

Chao. X.B., Jia,Y. , Shields, D. and Wang, S.S.Y.(2007), Numerical modeling of water quality and sediment related processes, *Ecological Modelling*, 201, 385–397.

Chao, X., Jia, Y., and Wang, S.S.Y.(2009), 3D numerical simulation of turbulent buoyant flow and heat transport in a curved open channel, *Journal of Hydraulic Engineering*, Vol. 135, No.7, 554-563.

Cozar, A., Galvez, J.A., Hull, V., Garcia, C.M., and Loiselle, S.A. (2005). Sediment resuspension by wind in a shallow lake of Esteros del Ibera (Argentina): a model based on turbidimetry. *Ecological Modelling*, 186, 63-76.

Chapra, S.C., 1997. *Surface Water-Quality Modeling*, The Mcgraw-Hill Companies, Inc, New York.

Dyer, K.R.(1986). *Coastal and Estuarine sediment dynamics*, John Wiley & Sons Inc.

Gailani, J., Ziegler, C.K. and Lick, W. (1991). Transport of suspended solids in the Lower Fox River. *J. Great Lakes Res*., 17(4), 479-494.

Glenn, S.M. and Grant, W.D. (1987). A suspended sediment stratification correction for combined waves and current flows. *J.Geophys. Res*.,92(C8), 8244-8264.

Grant, W.D. and Madsen, O.S.(1979). Combined wave and current interaction with a rough bottom. *J.Geophys. Res*.,84(C4), 1797-1808.

Hamilton, D.P. and Mitchell, S.F. (1996). An empirical model for sediment resuspension in shallow lakes. *Hydrobiologia*, 317, 209-220.

Hamm, L. and Migniot, C. (1994). Elements of cohesive sediment deposition, consolidation, and erosion, *Coastal, Esturial, and Harbor Engineer's Reference Book*, M.B.Abbott and W.A.Price (Ed.), Chapman and Hall, London, pp 93-106.

Hawley, N. and Lesht, B.M.(1992). Sediment resuspension in Lake St.Clair. *Limnol. Oceanogr.*, 37(8), 1720-1737.

Huang, W. and Spaulding, M. (1995). 3D model of estuarine circulation and water quality induced by surface discharges. *Journal of Hydraulic Engineering*, 121(4), 300-311, 1995.

Jia, Y., Kitamura, T., and Wang, S.S.Y.(2001). Simulation scour process in a plunge pool with loose material. *J. Hydraul. Eng*., 127, 219-229.

Jia, Y., Scott, S., Xu, Y., Huang, S. and Wang, S.S.Y.(2005). Three-Dimensional numerical simulation and analysis of flows around a submerged weir in a channel bendway. *J. Hydraulic Engineering*, 131(8), 682–693.

Jin, K. R.,Hamrick, J. H., and Tisdale, T. (2000). Application of three dimensional hydrodynamic model for Lake Okeechobee. *J. Hydraulic Engineering*, 126(10), 758–771.

Jin, K.R., and Ji, Z.G. (2004). "Case study: modeling of sediment transport and wind-wave impact in Lake Okeechobee." J. Hydraulic Engineering, 130(11), 1055-1067.

Jin, K.R., and Sun D. (2007). Sediment resuspension and hydrodynamics in Lake Okeechobee during the late summer. *J. Engineering Mechanics*, 133(8), 899-910.

Hayter, E.J. (1983), *Prediction of Cohesive Sediment Movement in Estuarial Waters*, Ph.D. Dissertation, University of Florida, Gainesville, Florida, USA.

Kocyigit, M.B., and Kocyigit, O. (2004). Numerical study of wind-induced currents in enclosed homogeneous water bodies. *Turkish J. Engineering & Environmental Science*, 28, 207- 221.

Koutitas, C., and O'Connor, B., (1980). Modeling three-dimensional wind-induced flows. ASCE, *Journal of Hydraulic Division*, 106 (11), 1843-1865.

Krone, R.B. 1962. *Flume Studies on the Transport of Sediment in Estuarine Shoaling Processes*, Hydraulic Engineering Laboratory, University of California, Berkeley.

Lane, E.W. and Koelzer, V.A. (1953). Density of sediments deposited in reservoirs, *Report No.9, A study of Methods Used in Measurement and Analysis of Sediment Loads in Streams*, Engineering District, St.Paul, MN,USA.

Li, Y. and Mehta, A.J.(1998). Assessment of hindered settling of fluid mudlike suspensions. *J. Hydraulic Engineering*, 124(2), 176-178.

Lick, W. and Lick, J. (1988). Aggregation and disaggregation of fine-grained lake sediments. *J. Great Laks Res.*, 14(4), 514-523.

Liu, W.C. (2007). Modelling the effects of reservoir construction on tidal hydrodynamics and suspended sediment distribution in Danshuei River estuary, *Environmental Modelling & Software*, 22(11), 1588-1600.

Locke, M. A. (2004). Mississippi Delta Management Systems Evaluation Area: Overview of water quality issues on a watershed scale. M.T. Nett, M.A.Locke, and D.A.Penninngton (Ed.), *Water Quality Assessment in the Mississippi Delta: Regional Solutions, National Scope*. ACS Symposium Series 877, American Chemical Society, Washington, D. C.

Lou, J., Schwab, D.J., Beletsky, D. and Hawley, N. (2000). A model of sediment resuspension and transport dynamics in southern Lake Michigan. *Journal of Geophysical Research*, 105, (C3), 6591-6610.

Luettich, R.A., Harleman, D.R.F. and Somlyody, L. (1990). Dynamic behavior of suspended sediment concentrations in a shallow lake perturbed by episodic wind events. *Limnol. Oceanogr.*, 35(5), 1050-1067.

McConnachie, G. L. (1991). Turbulence intensity of mixing in relation to flocculation, *J. Environ. Eng.*, 117(6), 731-750.

Mehta, A.J. and Partheniades, E.(1975). An investigation of the depositional properties of flocculated fine sediment. *J. Hydraulic Research*, 13(4), 361-381.

Mehta, A.J. (1986). Characterization of cohesive sediment properties and transport processes in estuaries, *Estuarine Cohesive Sediment Dynamics*, A.J.Mehta (Ed.), Springer-Verlag, 290-325.

Nicholson, J. and O'connor B.A. (1986). Cohesive sediment transport model. *J. Hydraulic Engineering*, 112(7), 621-640.

Normant, C.L. (2000). Three-dimensional modeling of cohesive sediment transport in the Loire estuary. *Hydrol. Process*. 14, 2231-2243.

Partheniades, E.(1965). Erosion and deposition of cohesive soils. *J. Hydraulic Division*, ASCE, 91(HY1).

Rebich, R.A and Knight, S. S. (2001). The Mississippi Delta Management Systems Evaluation Area Project, 1995-99. *Mississippi Agriculture and Forestry Experiment Station, Information Bulletin 377*, Division of Agriculture, Forestry and Veterinary Medicine, Mississippi State University.

Rueda, F. J. and Schladow, S. G. (2003). Dynamics of large polymictic lake. II: Numerical Simulations. *J. Hydraulic Engineering*, 129(2), 92-101.

Shields, F. D. Jr., S. S. Knight, C. M. Cooper, and S. Testa. (2003). Use of acoustic Doppler current profilers to describe velocity distributions at the reach scale. *Journal of the American Water Resources Association*, 39, 1397–1408.

Stone, H. L. (1968). Iterative solution of implicit approximation of multidimensional partial differential equations. *SIAM (Soc. Ind. Appl.Math.) J. Numer. Anal*., 5, 530–558.

Stow, C. A., Roessler, C., Borsuk, M. E., Bowen, J. D., and Reckhow, K. H. (2003). Comparison of Estuarine Water Quality Models for Total Maximum Daily Load Development in Neuse River Estuary. *J. Water Resour. Plan. Manage*., ASCE, 129(4), 307-314.

Teeter A.M. et al. (2001). Hydrodynamic and sediment transport modeling with emphasis on shallow-water, vegetated area (lakes, reservoirs, estuaries and lagoons). *Hydrobiologia*, 444, 1-23.

Thomann, R.V. and Mueller J.A. (1988). *Principles of Surface Water Quality Modeling and Control*, Harper&Row Publication, New York.

Thorn,M.F.C.(1981). Physical processes of siltation in tidal channels. *Proc. Hydraulic Modelling Applied to Maritime Engineering Problems*, ICE, London, 47-55.

Tsanis, I.K. (1989). Simulation of wind-induced water currents. *J. Hydraulic Engineering*, 115(8), 1113-1134.

Van Rijn, L. C. (1989). *Handbook Sediment Transport by Currents and Waves*, Report H461, Delft Hydraulics.

Van Rijn, L.C. (1993). *Principles of Sediment Transport in River, Estuaries and Coastal Seas*, AQUA Publication, Amsterdam, Netherlands.

Willis, D. and Krishnappan, B.J.(2004). Numerical modelling of cohesive sediment transport in rivers. *Can. J. Civil Engineering*, 31, 749-758.

Wu, W. (2008). *Computational River Dynamics*, Taylor & Francis Group, London, UK.

Wu, W. and and Wang, S.S.Y.(2004). Depth-averaged 2-D calculation of tidal flow, salinity and cohesive sediment transport in estuaries. *Int. J. Sed. Res*., 19(3), 172-190.

Ziegler, C.K. and Nisbet, B.S.(1995). Long-term simulation of fine-grained sediment transport in large reservoir. *J. Hydraulic Engineering*, 121(11), 773-781.

Zhang, Y.X.(2002). *CCHE Mesh Generator User Manual*, Technical Report, The University of Mississippi.

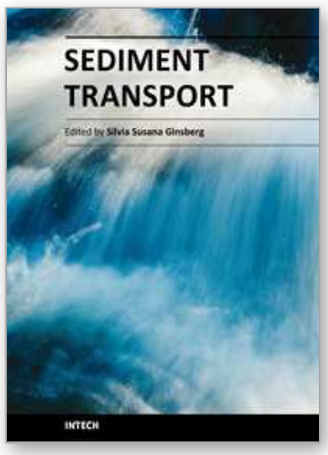

Sediment Transport

Edited by Dr. Silvia Susana Ginsberg

ISBN 978-953-307-189-3
Hard cover, 334 pages
Publisher InTech
Published online 26, April, 2011
Published in print edition April, 2011

Sediment transport is a book that covers a wide variety of subject matters. It combines the personal and professional experience of the authors on solid particles transport and related problems, whose expertise is focused in aqueous systems and in laboratory flumes. This includes a series of chapters on hydrodynamics and their relationship with sediment transport and morphological development. The different contributions deal with issues such as the sediment transport modeling; sediment dynamics in stream confluence or river diversion, in meandering channels, at interconnected tidal channels system; changes in sediment transport under fine materials, cohesive materials and ice cover; environmental remediation of contaminated fine sediments. This is an invaluable interdisciplinary textbook and an important contribution to the sediment transport field. I strongly recommend this textbook to those in charge of conducting research on engineering issues or wishing to deal with equally important scientific problems.

INTECH
open science | open minds

InTech Europe
University Campus STeP Ri
Slavka Krautzeka 83/A
51000 Rijeka, Croatia
Phone: +385 (51) 770 447
Fax: +385 (51) 686 166
www.intechopen.com

InTech China
Unit 405, Office Block, Hotel Equatorial Shanghai
No.65, Yan An Road (West), Shanghai, 200040, China
中国上海市延安西路65号上海国际贵都大饭店办公楼405单元
Phone: +86-21-62489820
Fax: +86-21-62489821

IntechOpen